IEEE Access
Multidisciplinary | Rapid Review | Open Access Journal

Received 9 November 2024, accepted 29 November 2024, date of publication 2 December 2024,
date of current version 11 December 2024.

Digital Object Identifier 10.1109/ACCESS.2024.3510522

RESEARCH ARTICLE

Matrix Pencil for RFID Collision Recovery

HAMED SALAH[1], REZA HASSANPOUR[1], AND GEORGI GAYDADJIEV[1,2], (Senior Member, IEEE)
[1]Bernoulli Institute for Mathematics, Computer Science and Artificial Intelligence, University of Groningen, 9700 AK Groningen, The Netherlands
[2]Department of Quantum and Computer Engineering, Delft University of Technology, 2628 CD Delft, The Netherlands

Corresponding author: Hamed Salah (h.s.h.kenawy@rug.nl)

The research is funded by Bernoulli Institute for Mathematics, Computer Science and Artificial Intelligence, University of Groningen.

ABSTRACT Collision recovery is considered one of the main potentials for improving bulk reading speed in the UHF radio identification (RFID) system. The collision occurs when two or more tags reply at the same time. State-of-the-art collision recovery algorithms rely on perfect channel state information (CSI), which is unrealistic. Moreover, these algorithms neglect the rate tolerance, that is, the uncertainty in the bit rate of the tag responses. This paper presents a novel algorithm to estimate all tag parameters, such as tag data rate, number of tags per slot, and CSI, using the Matrix Pencil Method (MPM). The proposed system is compatible with the existing EPCglobal Class-1 Gen-2 RFID standard. The accuracy of the proposed algorithm is evaluated with the different encoding schemes of the tag. The estimated parameters are forwarded to MIMO linear receivers to recover the colliding slots to speed up the identification process. The performance of the three linear receivers; Zero Forcing (ZF), Minimum Mean Square Error (MMSE), and Maximum Likelihood (ML) receivers, is evaluated when the CSI is estimated using the proposed algorithm. All receivers perform similarly due to their different sensitivity to the CSI estimation error. The proposed collision recovery system reduces the time for reading a bulk by at least 13% compared to the literature.

INDEX TERMS RFID, FSA, matrix pencil method, collision recovery, backscatter Rayleigh.

I. INTRODUCTION

Radio Frequency Identification (RFID) is a wireless communications-based technology that allows the automatic identification of objects. The number of RFID applications has skyrocketed in recent years, and this trend is projected to continue in the future. RFID technology is used in the logistics industry to identify and track physical goods that have a very large number of items using ultra-low-cost passive tags. EPCglobal Class-1 Gen-2 is the most widely used standard for such applications (EPC) [1]. This standard operates in the UHF band (that is, 868 MHz in Europe, 915 MHz in the USA) and allows the recognition of RFID tags up to approximately 10 m reading range [2]. In many real-life scenarios, hundreds of labeled objects may be located within the reading range. Tag responses should be scheduled using an access method based on frame-slotted ALOHA (FSA) [3]. According to FSA, all tags in the reading range are informed by the reader about the number of available slots referred to as the *frame length*, L. Then, each tag randomly attempts to reserve one of the available slots by answering with a random 16-bits number called RN16. The slots used by a single tag are called *successful slots* and can normally be decoded. If two or more tags reply within a single slot, a collision occurs, and the replies of the tags cannot be decoded [4]. Afterward, the reader has to try reading these colliding tags in a later frame. This automatically increases the reading time, which may be problematic in some applications. As a result, many strategies for recovering colliding slots have been presented. Nevertheless, the so-called Backscatter Link Frequency (BLF), i.e., the bit-rate of communication from the tags to the reader, is a problem within the EPCglobal Class-1 Gen-2 RFID standard [1]. Due to factors that cannot be avoided in real-world systems, the BLF can vary greatly. Low-cost RFID tags typically have a sluggish system clock for digital baseband operation, resulting in measurement errors for the parameters sent by the reader to determine the tag's BLF. Second, changes in the manufacturing process commonly affect the clock frequency of the tag, leading to fluctuations in the BLF. According to the EPCglobal standard, the permitted relative tolerance ranges from $\pm 4\%$ up to $\pm 22\%$, depending

The associate editor coordinating the review of this manuscript and approving it for publication was Renato Ferrero.

on the targeted bit rate. The majority of previous research on collision recovery for RFID systems assumes that the colliding tags have the same BLF and are also perfectly synced in time [5], [6]. Moreover, all or part of the colliding tags parameters, such as the number of tags per colliding slot and channel coefficients, are assumed to be perfectly known during the identification process. Hence, the motivation of this work is to design a collision recovery system that can estimate all the parameters of the tags during the inventory phase and that is compatible with the EPCglobal Class-1 Gen-2 RFID standard [1]. These tags parameters can be used in recovering the colliding slots to speed up the reading process. The main contributions to this work are as follows:

- A novel spectrum analysis technique using matrix pencil method is proposed to estimate tags parameters accurately;
- Careful performance evaluation of the proposed parameter estimation technique in the presence of tags collision;
- A novel channel coefficient estimation performance study is presented, considering the effect of the modulation scheme and the number of colliding tags per slot.
- Combining the proposed parameters estimation method with state-of-the-art tags collision recovery receivers to examine its performance.

The paper is organized as follows: Section II introduces the relevant related work. Section III describes the assumed data model, including the channel model, signal definition, and tag rate tolerance model. The estimation of tag parameters using a matrix pencil using the BLF tolerance is proposed in Section IV. In Section V, the state-of-the-art collision recovery linear receivers are introduced. The simulation results are discussed in Section VI. Finally, conclusions are drawn in Section VII.

II. RELATED WORK

Many collision recovery techniques have been proposed to speed up the identification process. Carroccia and Maselli [7] proposed TIANC (Tag Identification Analog Network Coding). They combined multiple receiver antennas with tree-slotted Aloha. Furthermore, they assumed that the tags generated a new child frame for each collision slot. This approach increases the tag complexity and, hence, the hardware costs. In addition, their approach is incompatible with the existing UHF RFID standard. Guo et al. Similarly, an orthogonal coset identification (OCSID) is proposed in [8]. The proposed approach requires a modification in the tag to ensure orthogonality between the tag responses in the inventory phase. Reference [9] proposed a channel estimation technique that could be used to estimate the channel of up to eight collided tags per slot. This channel estimation technique is used in [10] to separate the tags. However, this approach is again not compatible with the EPCglobal Class-1 Gen-2 RFID standard, and the tolerance of BLF is not taken into account. The authors in [11] proposed a collision recovery technique utilizing rate tolerance. In this algorithm, the Fast Fourier Transform (FFT) is used to analyze the preamble of the tag reply to estimate the data rate of the strongest tag reply. In addition, the probability of the capture effect is enhanced using a correlation receiver. In [12], the cardinality estimation of the tags is combined with a channel estimation technique to recover collisions. The performance of the proposed algorithm drastically degrades if the rate tolerance is greater than 10%. In [13], a maximum likelihood receiver is proposed to recover non-synchronized collided tags. The introduced algorithm has limited performance because it can only recover two collided tags at most. Another related work [6] proposes a collision recovery algorithm with the aid of machine learning. The proposed algorithm does not consider the rate variations between the collided tags, which will significantly affect their model. The rate tolerance is considered in [14]. The authors proposed an adaptive neural network to separate the collision tag signal. However, the performance of the introduced algorithm deteriorates as the rate tolerance increases. The authors in [15] suggested an anti-collision algorithm in combination with a receiver with multiple receiving antennas. The algorithm improves the identification speed by 50%, when 4 receiving antennas are used. A multi-user MIMO collision recovery system is proposed in [16]. The authors exploited multiple receive antennas to recover collided tag data and perform channel estimation. In addition, channel estimates are used to precode reader acknowledgment signals from multiple transmit antennas into spatial channels so that the tags receive fully separated acknowledgments. The reader needs a sampling rate of 30 MSPS which is four times higher the proposed one. In [17], the clustering method is proposed that uses Monte Carlo-based maximum posteriori probability estimation (MPPE-M-C) to resolve the collision signal. the proposed algorithm does not require prior knowledge of the number of clusters and iterative calculations.

III. DATA MODEL

Before going into the details of the proposed algorithm, let us first describe the data model. Fig. 1 shows the assumed data model for a bi-static[1] RFID reader with a single tag. The following subsections describe the channel model between the RFID reader and a single tag, and then it is extended to a multi-tag. Additionally, the tag signal is defined.

A. CHANNEL MODEL

The transmit antenna (TX) radiates the signal $x(t)$. This signal contains the continuous wave needed to power the tags and also the commands that comprise the information from the reader to the tag. The continuous wave may have a power higher than 1 W, as this signal is used by passive tags to obtain the required energy. The tag received power is considered time-invariant, which is a realistic assumption based on [18]. The signal at the input of the receive antenna (RX) is $y(t) \in \mathbb{C}$. The signal $y(t)$ is the complex baseband representation of the tag reply [19]. It constitutes a direct coupling

[1]The reader uses separate antennas for transmission and reception.

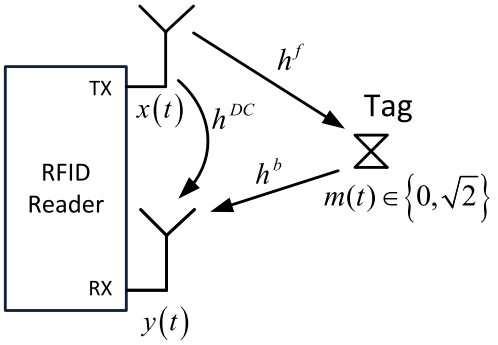

FIGURE 1. The assumed RFID bi-static reader data model.

of the transmit antenna to the RX antenna, which we can describe with the coupling coefficient $h^{DC} \in \mathbb{C}$. Furthermore, we have the signal of the tag response. For sending data to the reader, the tag modifies its antenna impedance between two states. In the presence of the continuous wave emitted by the reader, this change of the antenna impedance causes a signal back-scattering to the reader. Mathematically, this can be described using the forward channel coefficient $h^f \in \mathbb{C}$ to model the path from the TX antenna to the tag and using the backward channel $h^b \in \mathbb{C}$ for modeling the path from the tag to the RX antenna. Moreover, we have the state of the tag, which can be modeled as $m(t) \in \{0, \sqrt{2}\}$[2] [11]. Hence, the signal $y(t)$ can be expressed as:

$$y(t) = \left(h^{DC} + h^b \cdot m(t) \cdot h^f\right) \cdot x(t) + n(t) \tag{1}$$

where $n(t)$ is complex additive white Gaussian noise with zero mean and variance σ_n^2. Additionally, the channel effects are purely multiplicative, i.e. the channel is considered as non-frequency selective [19]. This assumption is fully justified as the used bit rate is low enough concerning the expected delay spread of the channel [19]. The tag reply data rate varies between 5 kbps and 640 kbps. Generally, the tag has more impact on the signal $y(t)$ than just an on-off-keying modulation. For example, the tag will reflect an electromagnetic wave to the reader in both possible states of $m(t)$ [11]. However, we simply model the default state as part of h^{DC}. Therefore, this leads to the description using on-off-keying [20]. This is valid for all modulations mentioned in the EPCglobal Class-1 Gen-2 RFID standard, i.e., ASK (amplitude shift keying), or more precisely, on-off-keying and PSK (phase shift keying) [1]. The actual modulation scheme is then modeled as part of the return channel h^b. Now, a further simplification can be proposed to (1). In this paper, we focus on the communication from the tag to the reader. The reader transmits a continuous wave during this communication, which can be safely modeled as $x(t) = 1$. Furthermore, the h^{DC} component can be estimated and removed in the front-end of the reader [21]. As a result, we obtain the following:

$$y(t) = h^b \cdot m(t) \cdot h^f + n(t) \tag{2}$$

[2]The factor $\sqrt{2}$ is to have unity signal power.

The resulting channel, consisting of two multiplied channel coefficients, is called the back-scatter channel. In the case of a bi-static reader, modeling both coefficients as independent complex Rayleigh channels is a realistic assumption [22]. In the case of multiple tags and a reader employing a single receiver antenna, we can extend (2) to vectors. This leads to:

$$y(t) = \mathbf{h}^b \cdot \left(\mathbf{m}^T(t) \odot \mathbf{h}^{fT}\right) + n(t) \tag{3}$$

where $(.)^T$ is the vector transpose, and $\odot$ is the Hadamard product. Furthermore, $\mathbf{h}^b \in \mathbb{C}^{N_c}$, $\mathbf{m}(t) \in \{0, \sqrt{2}\}^{N_c}$, $\mathbf{h}^f \in \mathbb{C}^{N_c}$, and N_c defines the number of colliding tags per slot.

Equation (3) can be extended in case of multiple tags and multiple receive antennas for the reader to be

$$\begin{bmatrix} y_1 \\ \vdots \\ y_R \end{bmatrix} = \begin{bmatrix} h_{11} & \cdots & h_{1N_c} \\ \vdots & \ddots & \vdots \\ h_{R1} & \cdots & h_{RN_c} \end{bmatrix} \begin{bmatrix} m_1 \\ \vdots \\ m_{N_c} \end{bmatrix} + \begin{bmatrix} n_1 \\ \vdots \\ n_R \end{bmatrix} \tag{4}$$

where R is the number of receive antennas, and $h_{ij} = h_i^b \cdot h_j^f$. For simplicity, (4) can be written as

$$\mathbf{y} = \mathbf{H} \cdot \mathbf{m} + \mathbf{n} \tag{5}$$

where $\mathbf{y}$ is the received tag replies vector, $\mathbf{H}$ is the channel matrix, $\mathbf{m}$ is the transmitted tag replies vector, and $\mathbf{n}$ is the receiver AWGN vector [18].

B. TAG SIGNAL DEFINITION

Based on the EPCglobal standard [1], the pulse shapes of the response to the tag $s_n(t)$ follow the FM0 (biphase space) or Miller encoding. As FM0 encoding offers a higher bit rate, most of the readers prefer to use it as an encoding scheme [23]. The pulse shapes $s_n(t)$ for the symbols are selected from four possible shapes as shown in Fig. 2a, where $s_1(t)$ and $s_4(t)$ represent data-1 and $s_2(t)$ and $s_3(t)$ represent data-0. As shown in the state diagram in Fig. 2b, the symbols feature a level transition at each boundary. For example, the pulse $s_2(t)$ can only be followed by $s_2(t)$ or $s_1(t)$, but not by the symbols $s_3(t)$ or, $s_4(t)$ to guarantee a level transition between the symbols [1]. Based on the standard, the nominal symbol duration T is the inverse of the BLF, that is, $T = 1/\text{BLF}$. The tag response constitutes a preamble, followed by the payload. The shape and length of the preamble depend on the encoding scheme. As depicted in Fig. 2c, FM0 has two versions of the preamble according to the reader's choice. The short version has a length of 6 bits. The extended version has 12 additional leading zeros (dotted lines) in front of the 6 bits that are also used in the short version [1]. Fig. 3a and Fig. 3b show the basis functions and the state diagram in the case of Miller encoding. The baseband Miller inverts its phase between two data-0s in sequence. It also places a phase inversion in the middle of a data-1 symbol. The state labels, $s_1(t) \cdots s_4(t)$, indicate the four possible Miller-encoded symbols, represented by the two phases of each of the Miller basis functions. The transmitted waveform is the baseband waveform multiplied by a square wave at M times the symbol rate. Like FM0, the tag-to-reader subcarrier

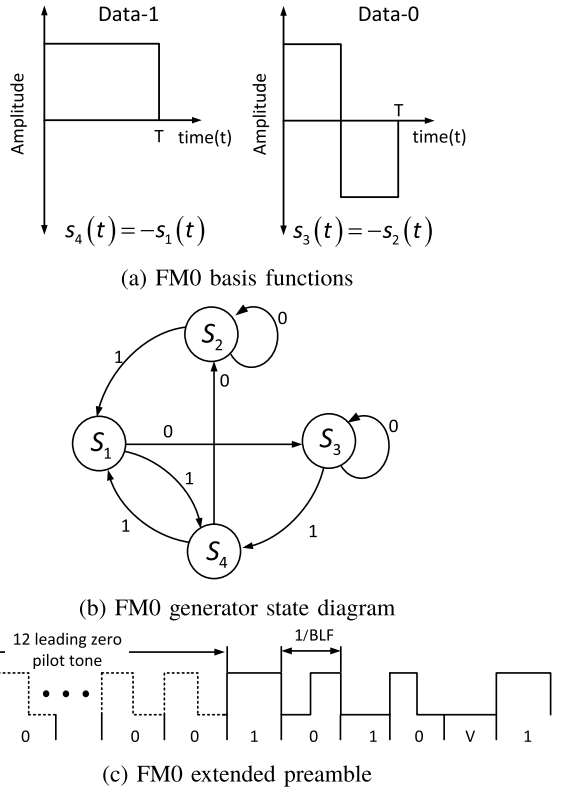

(a) FM0 basis functions

(b) FM0 generator state diagram

(c) FM0 extended preamble

FIGURE 2. FM0 encoding scheme.

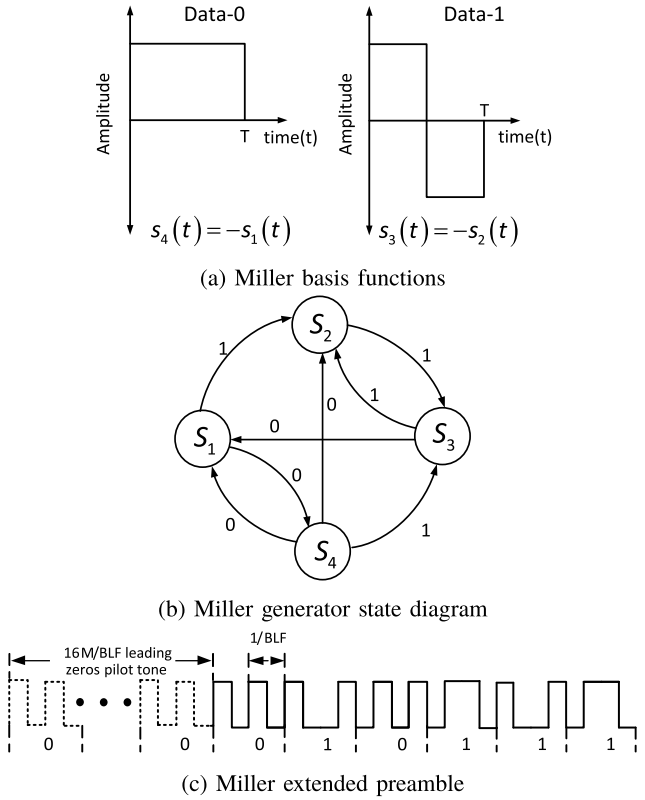

(a) Miller basis functions

(b) Miller generator state diagram

(c) Miller extended preamble

FIGURE 3. Miller encoding scheme.

signaling begins with one of two possible preambles. One preamble has an extended pilot tone of length $16M/\text{BLF}$, as shown in Fig. 3c, and the other has a pilot tone of length $4M/\text{BLF}$.

C. TAG RATE TOLERANCE

An important property of tags replies is the rate tolerance in their BLFs. At the beginning of the reading process, the reader sends the so-called Query command to all tags in the interrogation area [1]. This command contains all the required information to configure the tags, e.g., whether they use the extended preamble or whether they should use FM0 or Miller encoding of the data. Tags are designed with ultra-low cost in mind and cannot accurately estimate BLF from the preamble parameters of the query command [11]. The allowed BLF tolerance depends on the nominal values of the parameter settings [1]. The maximum tolerance varies between $\pm 4\%$ at $40\,\text{kHz} \leq \text{BLF} < 107\,\text{kHz}$, and $\pm 22\%$ at $320\,\text{kHz} \leq \text{BLF} < 640\,\text{kHz}$. The actual BLF can be described as:

$$\text{BLF} = \text{BLF}_{\text{nominal}} \cdot \beta \tag{6}$$

where β is a normally distributed random variable with a mean μ equal to one and a standard deviation σ equal to (maximum absolute tolerance)/3 to force the tail of the distribution to end at the maximum absolute tolerance.

For example, if the tolerance varies between $\pm 20\%$, the standard deviation is $\sigma = 0.2/3$. Hence, the total distribution of the BLF has a mean equal to $BLF_{nominal}$, and the tails end at $\text{BLF}_{\text{max}} = \text{BLF}_{\text{nominal}}\,(1 + 3 \cdot \sigma)$ and $\text{BLF}_{\text{min}} = \text{BLF}_{\text{nominal}}\,(1 - 3 \cdot \sigma)$ [11].

IV. PARAMETERS ESTIMATION USING MATRIX PENCIL

The Matrix Pencil Method (MPM) is a direct data domain method that can estimate the parameters of exponentially damped and undamped sinusoid signals in noise [24]. In this work, we will deal with undamped signals, and the response signal of the tag $y_p(t)$ is assumed to be the sum of exponentials in the noise as shown in (7).

$$y_p(t) = \sum_{j=1}^{N_c} a_j \cdot e^{i(\omega_j t + \theta_j)} + n(t) \tag{7}$$

where the parameters a_j, θ_j, and ω_j are the amplitude, the phase, and the angular frequency of the jth tag signal. The signal $n(t)$ is complex additive white Gaussian noise with zero mean and variance σ_n^2.

A. MPM DESCRIPTION

Estimation of the tag parameters using MPM is shown in Figure 4 and can be summarized in the following steps:

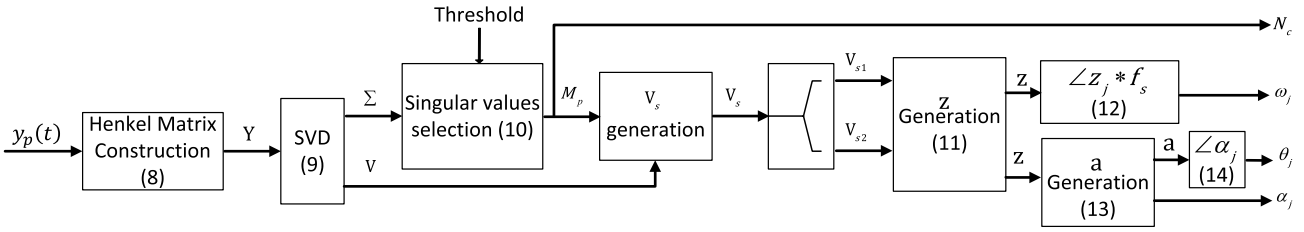

FIGURE 4. Block diagram of the MPM.

- A Henkel matrix $\mathbf{Y}$ can be constructed as follows:

$$\mathbf{Y} = \begin{bmatrix} y_p(0) & y_p(1) & \cdots & y_p(L-1) \\ y_p(1) & y_p(2) & \cdots & y_p(L) \\ \vdots & \ddots & & \vdots \\ y_p(N-L) & y(N-L+1) & \cdots & y_p(N-1) \end{bmatrix} \tag{8}$$

  where N is the number of samples of the signal y_p and L is called the pencil parameter. It should be between $\frac{N}{3}$ and $\frac{N}{2}$ for effective noise filtering [24].
- After Singular Value Decomposition (SVD), (8) can be written as

$$\mathbf{Y} = \mathbf{U}\Sigma\mathbf{V}^H \tag{9}$$

  where $\mathbf{U}$ and $\mathbf{V}$ are unitary matrices whose columns are the left and right singular vectors of $\mathbf{Y}$, respectively. The matrix Σ contains the singular values λ_j of $\mathbf{Y}$ located on its main diagonal, and H is the Hermitian of the matrix.
- In this step, N_c major singular values are selected to form a matrix $\Sigma_\mathbf{s}$

$$\Sigma_\mathbf{s} = \mathtt{diag}\left(\lambda_1, \lambda_2, \ldots, \lambda_{M_p}\right), M_p < \mathtt{min}\left(N-L, L\right) \tag{10}$$

  where $\frac{\lambda_{M_p}}{\lambda_1} \geq \mathtt{Threshold}$. If the threshold is well optimized, $M_p = N_c$. The threshold can be calculated by estimating the signal-to-noise ratio (SNR) of the composite signal. The SNR can be estimated from the continuous wave (CW) before the tag response [25], [26].
- The matrix $\mathbf{V}_s$ can be generated by selecting the first M_p rows of matrix $\mathbf{V}$.
- The matrices $\mathbf{V}_{s1}$ and $\mathbf{V}_{s2}$ can be generated by deleting the last and first rows of the matrix $\mathbf{V}_s$, respectively.
- The poles of the vector $\mathbf{z}$ that is used to estimate the signal parameters are:

$$\mathbf{z} = \mathtt{Eigenvalues}\left(\left\{\mathbf{V}_{s1}^H\right\}^\dagger \mathbf{V}_{s2}^H\right) \tag{11}$$

  where † is the pseudo-inverse of the matrix.
- From the vector $\mathbf{z}$, the signal parameters can be calculated as follows:

$$\omega_j = \angle z_j * f_s, \tag{12}$$

$$\mathbf{a} = \begin{bmatrix} 1 & 1 & \cdots & 1 \\ z_1 & z_2 & \cdots & z_{M_p} \\ z_1^2 & z_2^2 & \cdots & z_{M_p}^2 \\ \vdots & & \ddots & \\ z_1^{M_p-1} & \cdots & & z_{M_p}^{M_p-1} \end{bmatrix} \begin{bmatrix} y(0) \\ y(1) \\ y(2) \\ \vdots \\ y\left(M_p-1\right) \end{bmatrix}, \tag{13}$$

$$\theta_j = \angle a_j \tag{14}$$

where f_s is the sampling frequency.

B. COMPLEXITY ANALYSIS

Generally, in all MP methods, the most computationally expensive step is to estimate the signal subspace, which requires the SVD of a data matrix. According to [27] and [28], the MPM used requires $8 \cdot (N-L+1)^2 \cdot L + 104 \cdot L^3$ complex multiplications. The complexity of the transformation of the data matrix is negligible [27]. However, some other MPM methods, such as the Unitary Matrix Pencil (UMP), Single Invariance Beamspace Matrix Pencil (SBMP), and Multiple Invariance Beamspace Matrix Pencil (MBMP) methods, have less complexity while retaining a comparable estimation accuracy [27]. Comparison of performance and complexity between different MP methods is not the focus of this work.

C. RFID READER WITH PARAMETERS ESTIMATION

As it is clear from the previous discussion, the MPM can be used to estimate the parameters for a summation of pure exponentials. However, the preamble of the tag reply is a square wave. Hence, a preprocessing step is needed for the tag reply before applying the MPM to the preamble.

Fig. 5 shows the proposed RFID reader that has parameter estimation capability. To explain this model, we need to rewrite (3).

Assume that the reader signal $x(t)$ that powers the tag can be expressed as

$$x(t) = A\sin(\omega_c t) \tag{15}$$

where ω_c is the carrier frequency and A is the amplitude of the continuous wave $x(t)$. Based on (3), the jth tag reply can be written as

$$y_j(t) = A\left|h_j^f\right| \cdot \left|h_j^b\right| \cdot m_j(t)\sin\left(\omega_c t + \theta_j^f + \theta_j^b\right) + n(t) \tag{16}$$

where θ_j^f, and θ_j^b are the phases of the forward and backward channels for the jth tag, respectively. It is clear from (16),

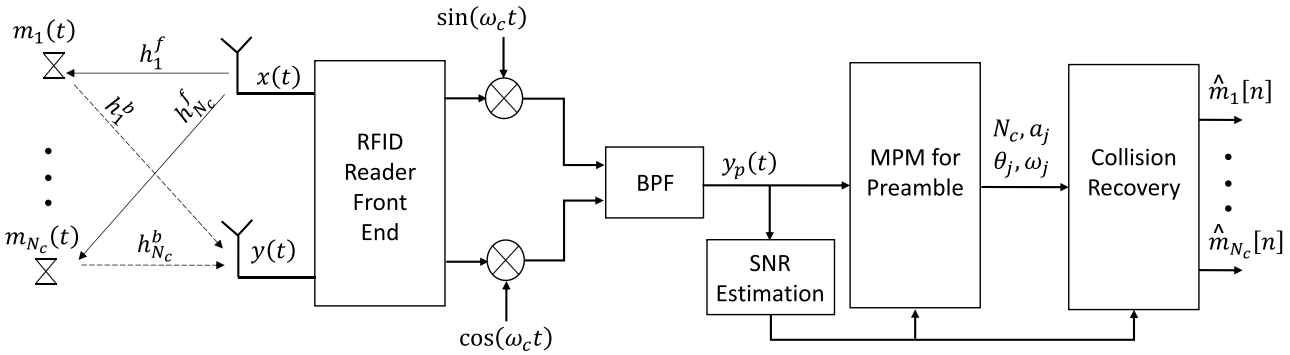

FIGURE 5. Block diagram of the proposed RFID reader model with parameters estimation using MPM.

that the parameters of the received tag reply signal cannot be estimated using MPM because $m_j(t)$ is not a pure sinusoidal signal. After down-converting the signal to the baseband and passing through a narrow-band pass filter (BPF), the whole received signal $y_p(t)$ can be written as

$$y_p(t) = \sum_{j=1}^{N_c} \frac{A}{2} \cdot \left|h_j^f\right| \cdot \left|h_j^b\right| \cdot \sin\left(\omega_j t + \theta_j^f + \theta_j^b + \theta_{bp}\right) + n_{bp}(t) \tag{17}$$

where θ_{bp} is the phase of the BPF, ω_j is the angular BLF of the jth tag, and $n_{bp}(t)$ is the narrow-band version of the noise signal $n(t)$. By using the trigonometric rules, (17) can be written as

$$\begin{aligned} y_p(t) = &\sum_{j=1}^{N_c} \frac{A}{4} \cdot \left|h_j^f\right| \cdot \left|h_j^b\right| \\ &\cdot \left(e^{i\left(\omega_j t + \theta_j^f + \theta_j^b + \theta_{bp} + \frac{\pi}{2}\right)} - e^{-i\left(\omega_j t + \theta_j^f + \theta_j^b + \theta_{bp} - \frac{\pi}{2}\right)}\right) \\ &+ n_{bp}(t) \end{aligned} \tag{18}$$

It is clear from (18), that the pencil signal $y_p(t)$ is a summation of pure exponential signals; hence, its parameters can be estimated using MPM. These parameters are the angular frequency of the backscatter link of each tag, ω_j, the amplitude of the channel, $\left|h_j^f\right| \cdot \left|h_j^b\right|$, and the channel phase added to it, the bandpass filter phase, $\theta_j^f + \theta_j^b + \theta_{bp}$. The phase of the band-pass filter, θ_{bp} is known from the phase response of the filter. Hence, it can be subtracted from the overall estimated phase. Using this channel state information (CSI), colliding tags can be recovered by linear receivers that need to have CSI knowledge, such as the Maximum Likelihood (ML) receiver, the Minimum Mean Square Error (MMSE) receiver, and the Zero Forcing (ZF) receiver. However, the proposed algorithm can be combined with any other MIMO receiver.

V. COLLISION RECOVERY RECEIVERS

The objective of any multiple antenna receiver is to obtain an estimate of the modulation signal of tags, $\hat{m}$, from the given received data in $\mathbf{y}$ over AWGN with noise variance σ_n^2, through channel $\mathbf{H}$ as described in (5). The transmitted vector $m \in A$, where A is the set of possible transmit vectors. Many types of multiple antenna receivers can be used in collision recovery [11]. Some of them are simple, such as the ZF receiver and the MMSE receiver. However, these receivers have poor performance compared to the optimal ones. Another receiver, Ordered Successive Cancellation, has a slightly higher complexity than the previous ones but has better performance [23]. The optimum receiver is the ML receiver. This receiver gives the optimum performance, but its complexity is much higher than all other receivers. In this work, we will focus on the ZF, MMSE, and ML receivers.

A. ZERO FORCING RECEIVER

To separate the signal components by exploiting multiple receive antennas, we first explain the well-known zero-forcing (ZF) receiver [29]. It is a simple linear receiver that inverts the channel transfer matrix $\mathbf{H}$ by calculating the pseudo-inverse of it. According to [29] and (5), the estimated vector $\hat{m_{ZF}}$ for the ZF receiver is calculated according to

$$\hat{\mathbf{m}}_{ZF} = \left(\mathbf{H}^H \mathbf{H}\right)^{-1} \mathbf{H}^H \cdot \mathbf{y} \tag{19}$$

The ZF receiver perfectly separates the co-channel signals of the vector $\mathbf{y}$. The ZF receiver performs well in a high signal-to-noise ratio (SNR) regime, whereas in a low SNR regime, there is a significant noise enhancement. The zero forcing criteria have the disadvantage that the inverse filter may excessively amplify the noise at frequencies where the folded channel spectrum has high attenuation. Therefore, the ZF equalizer suffers from noise enhancement, since it focuses on canceling the effects of the channel response at the expense of enhancing the noise.

B. MINIMUM MEAN SQUARE ERROR RECEIVER

As discussed earlier, the ZF receiver suffers from a noise enhancement due to the inversion of the channel matrix. The Minimum Mean Square Error (MMSE) receiver considers both interference and noise and balances the error. Following [29], the MMSE estimate of the signal vector $\hat{\mathbf{m}}_{MMSE}$ is

obtained according to

$$\hat{\mathbf{m}}_{MMSE} = \mathbf{H}^H \left(\mathbf{H}^H \mathbf{H} + \sigma_n^2 \cdot \mathbf{I}\right)^{-1} \cdot \mathbf{y} \tag{20}$$

where $\mathbf{I}$ is $R \times R$ the identity matrix and $\sigma_n^2 \cdot \mathbf{I}$ is the covariance matrix of the noise vector $\mathbf{n}$ in (5). The MMSE receiver is less sensitive to noise at the cost of reduced signal separation quality.

C. MAXIMUM LIKELIHOOD RECEIVER

As stated previously, the ML receiver is the optimum collision recovery receiver. It has the desirable property that it minimizes the probability of error P_e given by

$$P_e \triangleq \Pr\left(\mathbf{m} \neq \hat{\mathbf{m}}\right) \tag{21}$$

Minimizing the probability of error is equivalent to maximizing the probability of correctly estimating $\mathbf{m}$, i.e., $\Pr\left(\mathbf{m} = \hat{\mathbf{m}} \mid \mathbf{y}, \mathbf{H}\right)$. To maximize the probability of correct estimation, we have to maximize the probability density function of $\mathbf{y}$ given by $\mathbf{m}$ and $\mathbf{H}$, $\Pr(\mathbf{y} \mid \mathbf{m}, \mathbf{H})$ which is given by [29]

$$\Pr(\mathbf{y} \mid \mathbf{m}, \mathbf{H}) = \frac{1}{\pi^R \sigma_n^{2R}} exp\left(-\frac{\|\mathbf{y} - \mathbf{H}\mathbf{m}\|^2}{\sigma_n^2}\right) \tag{22}$$

Equation (22) is referred to as the ML criterion, and the detected signal is given by

$$\hat{\mathbf{m}}_{ML} = \arg\max_{\mathbf{m} \in A} \Pr(\mathbf{y} \mid \mathbf{m}, \mathbf{H}) = \arg\min_{\mathbf{m} \in A} \|\mathbf{y} - \mathbf{H}\mathbf{m}\|^2 \tag{23}$$

where $\mathbf{m} = \left[m_1 m_2 \cdots m_{N_c}\right]^T$.

VI. SIMULATION RESULTS

In this section, the simulation results are discussed to show the following:

- The precisions of the proposed RFID tag parameters estimation technique using BLF tolerance. These are shown in Figures 6 to 9.
- The identification performance of the collision recovery receiver in Figures 10 to 14.
- The reading time of the proposed receiver using different tolerance values in Fig. 15
- A throughput comparison between the proposed algorithm and the state of the art in Table 1

In our experiments, the model of (3) and (5) is used. The backscatter (also called double Rayleigh) channel is mainly used. It is the commonly assumed model for passive UHF RFID systems [22], [30]. Using this model, the forward and backward channels are derived from independent Rayleigh distributions. For comparison of performance, the SNR is used as a performance metric. In all simulations, the noise power corresponds to a sampling frequency f_s of 8 MHz with a nominal BLF = 640 kHz. According to [1], the maximum rate tolerance at such a data rate is ±15%. Furthermore, the expected average signal level is normalized to one. The BLF tolerance follows a normal distribution, as described in (6). In all simulations, a frame of 500 slots is used, and they have the same number of colliding tags. Finally, for each encoding scheme, the extended preamble is assumed.

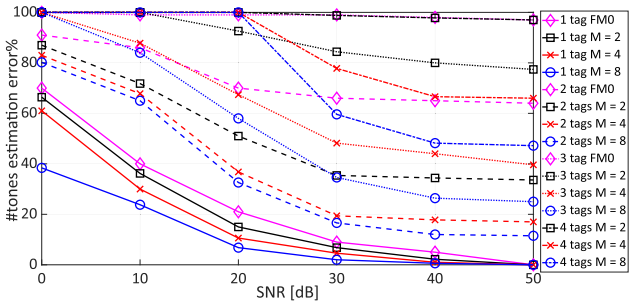

FIGURE 6. Number of tags per slot estimation error for different tag modulation schemes when the proposed MPM algorithm is used.

A. MPM PARAMETERS ESTIMATION ACCURACY

Figures 6 to 9 show the performance of estimating tags replies parameters using MPM when different encoding schemes are used. Fig 6 shows the number of tags per slot estimation error versus the SNR of the received replies. Through the simulations, the slot is erroneous if the estimated number of tags is not equal to the actual one. It is clear that as the number of tags per slot increases, the estimation error also increases. Moreover, when the preamble becomes longer by moving from FM0 modulation to Miller modulation, the performance of the estimation improves because the number of samples used by MPM for parameter estimation increases. Therefore, Miller with $M = 8$ always has the best estimation performance. The performance of the BLF estimation is shown in Figure 7. The BLF estimation error is calculated as follows:

- BLF estimation error per slot $= \sum_{N_c} \left| \frac{\text{estimated BLF} - \text{actual BLF}}{\text{actual BLF}} \right|$

Afterward, the error is averaged over the total number of slots. Similarly, performance improves as M increases. Furthermore, the performance of the estimation algorithm is limited when FM0 is used, especially when the number of tags per slot is greater than two. Therefore, the performance when two tags collide starts from 10 dB because, less than this value, FM0 has a very high error value. The same applies when three tags collide. Moreover, there is no estimation error curve for four colliding tags when FM0 is used. This is considered a limitation of the proposed technique. Figures 8 and 9 illustrate the error in estimating the amplitude and phase of the channel for each tag per slot. The amplitude and phase estimation errors are calculated using the same procedure as used in the BLF estimation error calculation.

B. COLLISION RECOVERY RECEIVERS PERFORMANCE

Figures 10 and 11 show the performance of the ZF receiver in recovering two and three colliding tags per slot, respectively. To be able to recover N_c tags per slot, the number of receive antennas has to be greater than or equal to N_c. Therefore, Figure 10 shows results for two, three, and four antennas. But Figure 11 has only results for three and four antennas.

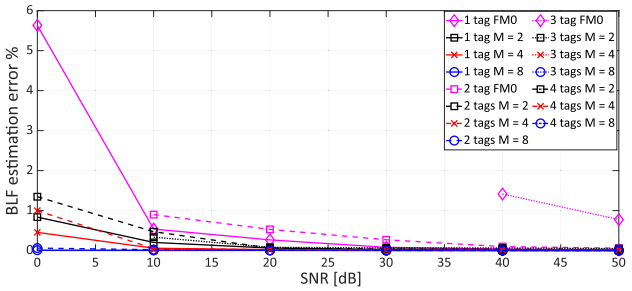

FIGURE 7. BLF per tag reply estimation error for different tag modulation schemes when the proposed MPM algorithm is used.

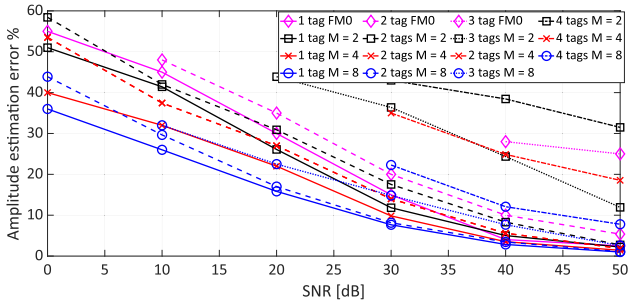

FIGURE 8. Channel amplitude estimation error of each tag reply for different tag modulation schemes when the proposed MPM algorithm is used.

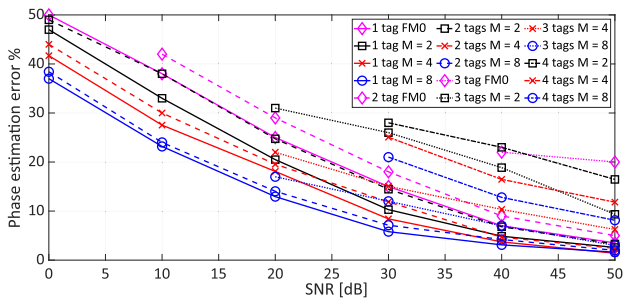

FIGURE 9. Channel phase estimation error of each tag reply for different tag modulation schemes when the proposed MPM algorithm is used.

The packet error rate (PER) is used as a performance metric where the packet is considered erroneous if it has a one-bit error. The packet here is the RN16 of the tag. The black square-marked curves represent the performance when the CSI is perfectly known; hence the modulation scheme is mentioned beside the legend of these curves. However, the other curves represent the performance when the CSI is estimated using the proposed MPM. It is clear that performance improves as the number of antennas increases and also as M increases because the performance of CSI estimation improves.

Similarly, Figures 12 and 13 show the performance of recovering two and three colliding tags per slot when using the MMSE receiver. The simulations illustrate that the performance of the MMSE receiver is slightly better than that of the ZF receiver, even at low SNR values. Although there

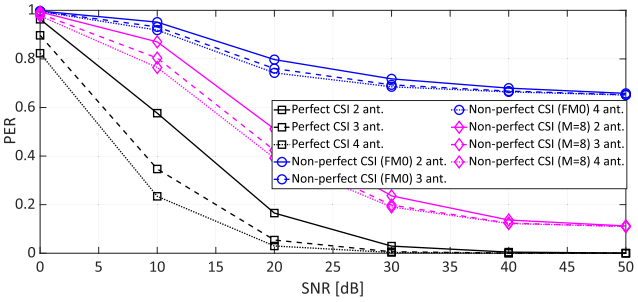

FIGURE 10. PER versus SNR of the multiple receive antennas ZF receiver for two colliding tags per slot.

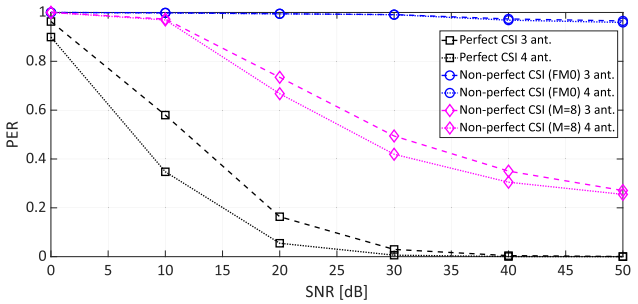

FIGURE 11. PER versus SNR of the multiple receive antennas ZF receiver for three colliding tags per slot.

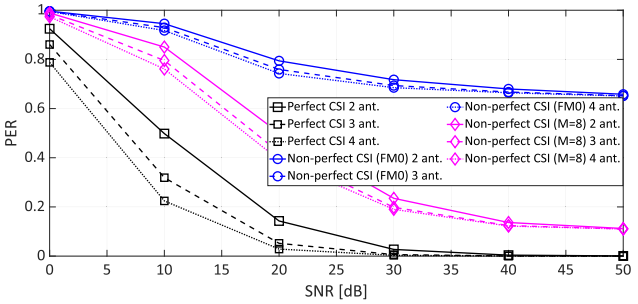

FIGURE 12. PER versus SNR of the multiple receive antennas MMSE receiver for two colliding tags per slot.

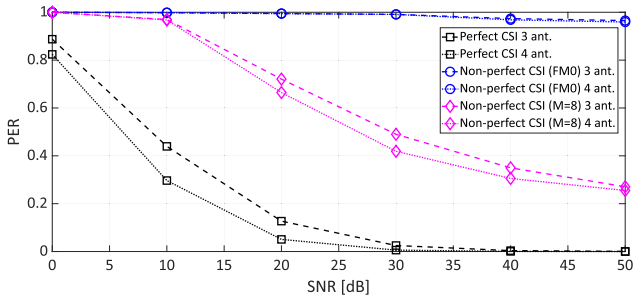

FIGURE 13. PER versus SNR of the multiple receive antennas MMSE receiver for three colliding tags per slot.

is a noise enhancement that the ZF receiver suffers from, the sensitivity of the MMSE receiver to the CSI estimation error is higher than that of the ZF receiver [31].

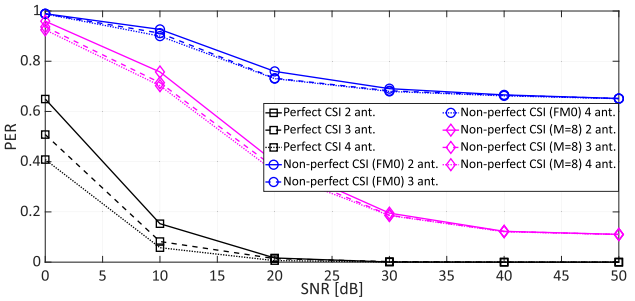

FIGURE 14. PER versus SNR of the multiple receive antennas ML receiver for two colliding tags per slot.

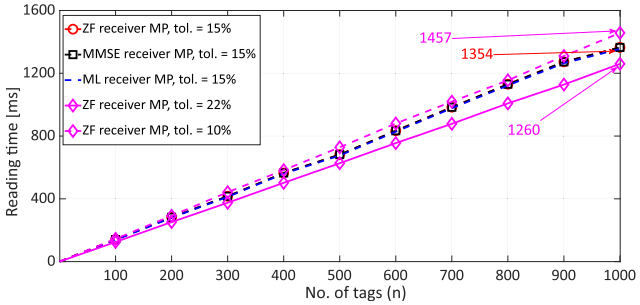

FIGURE 15. Average number of total slots needed to read all tags in the interrogation area when the proposed receiver with four receive antennas is used.

The performance of recovering two colliding tags using a multiple antenna ML receiver is simulated in Figure 14. Because of the BLF tolerance, the ML receiver can be used only to recover two colliding tags [13]. Similarly, the ML receiver does not show much improvement in performance because of its sensitivity to CSI estimation error [31]. Moreover, it has a much higher complexity than the ZF and MMSE receivers.

C. READING SPEED COMPARISON

Figure 15 shows the performance of the proposed algorithm using different types of receivers and with different values of rate tolerance. In this simulation, the performance metric is the reading time required to read the n tags in the interrogation area. The number of tags n is assumed to be perfectly known, and the frame length is optimized according to [25] and follows the frame length rule in the standard [1] for all techniques. In addition, all algorithms use four receiving antennas. Miller with $M = 8$ is used as a tag encoding scheme. In addition, an SNR of 50 dB is assumed. The simulation confirms previous PER simulations in which all receivers have the same performance. As explained above, the sensitivity of the ZF receiver to the CSI estimation error is less than that of the MMSE receiver, which is less than that of the ML receiver [31]. Therefore, all receivers have almost the same performance, as shown in Figure 15. The figure illustrates that at a rate tolerance of 15% [1], the proposed collision recovery receiver can read 1,000 tags using 1,354 slots. The figure also shows the proposed system performance at rate tolerances of ±10% and ±22%. Although the maximum tolerance allowed at the used data rate is ±15%, the tolerance can be stimulated to exceed that number [11]. It is clear that as the tolerance increases, the reading time decreases.

TABLE 1. Reading efficiency comparison.

Algorithm	Reading throughput (tags/slot)
MIMO DFSA [15]	0.53
Blind receiver [11]	0.643
ML receiver [13]	0.588
MPPE-M-C [3]	0.55
Conventional DFSA	0.36
Proposed	0.794

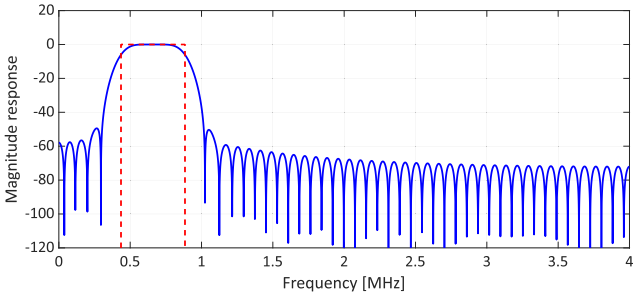

FIGURE 16. BPF magnitude response.

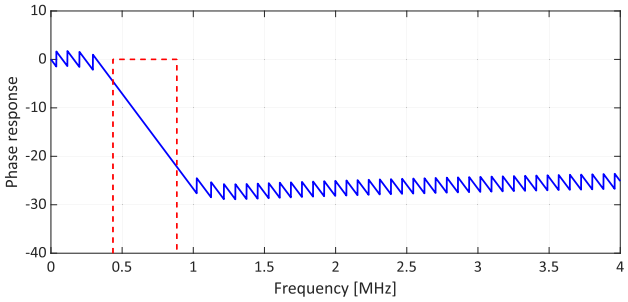

FIGURE 17. BPF phase response.

Table 1 shows the reading efficiency of the proposed algorithm and the ones that are proposed in [3], [11], [13], [15], and [16], and the conventional DFSA [16]. The reading throughput is defined as the ratio of the needed number of tags to the needed number of slots to identify these tags. The proposed algorithm outperforms all algorithms by at least 13%.

VII. CONCLUSION

This paper presents a novel UHF RFID tag estimation parameter using MPM. The proposed algorithm utilizes the non-avoidable rate tolerance phenomenon to estimate tag parameters such as BLF, number of tags per slot, and CSI per frame. Due to the rate tolerance, the RFID tags deviate from the nominal data rate, which is caused by

the low-cost oscillators of the tags. This rate tolerance is employed to estimate not only the BLF of each tag but also other parameters that can be useful in tag collision recovery. To convert the received signal to a complex exponential, the signal must be filtered using BPF. Therefore, MPM can be used for parameter estimation. The performance of the proposed estimation algorithm is evaluated when different tag encoding schemes are used. Due to its long preamble, Miller with $M = 8$ has the lowest estimation error for all parameters. However, FM0 cannot be used when the number of tags per slot is greater than three. That is even at high SNR values. That can be considered the main drawback of the proposed technique. The MPM estimation algorithm is combined with MIMO linear receivers to be used in collision recovery. The estimated CSI of the proposed MPM is used by the ZF, MMSE, and ML receivers to recover the colliding slots. The simulations show that the MMSE receiver performs slightly better than the ZF receiver because of its sensitivity to CSI and SNR estimation errors. The same is true for the ML receiver, which is more sensitive to the CSI estimation error. Hence, all receivers have the same performance from a timing point of view. The simulation shows that the proposed receiver is faster than the receivers that were presented earlier by at least 13%. In addition, the proposed system is considered to be a complete collision recovery system that has a slot identification system. This is achieved by estimating the number of tags per slot. A BLF estimation algorithm is used in the decoding process. A CSI estimation algorithm that can be used for collision recovery.

APPENDIX

The used BPF in the system has the following specifications:

- Order = 100;
- Filter type is FIR;
- Lower cut-off, $F_{CL} = 435.64\,\text{kHz}$;
- Higher cut-off, $F_{CH} = 884.08\,\text{kHz}$;
- Sampling frequency, $F_s = 8\,\text{MHz}$;
- The window type is hamming. The filter has a unity-magnitude response in the pass band.

The filter has magnitude and phase responses as shown in figures 16 and 17.

REFERENCES

[1] *EPC Radio-Frequency Identity Protocols Generation-2 UHF RFID Standard*, Standard Release 2.1, EPCglobal, 2018.

[2] K. Finkenzeller, *RFID Handbook: Fundamentals and Applications in Contactless Smart Cards and Identification*. Hoboken, NJ, USA: Wiley, 2003.

[3] J. Su, Z. Sheng, C. Huang, G. Li, A. X. Liu, and Z. Fu, "Identifying RFID tags in collisions," *IEEE/ACM Trans. Netw.*, vol. 31, no. 4, pp. 1507–1520, 2023.

[4] D.-J. Deng, C.-C. Lin, T.-H. Huang, and H.-C. Yen, "On number of tags estimation in RFID systems," *IEEE Syst. J.*, vol. 11, no. 3, pp. 1395–1402, Sep. 2017.

[5] C. Angerer and M. Rupp, "Advanced synchronisation and decoding in RFID reader receivers," in *Proc. IEEE Radio Wireless Symp.*, Jan. 2009, pp. 59–62.

[6] T. Akyildiz, R. Ku, N. Harder, N. Ebrahimi, and H. Mahdavifar, "ML-aided collision recovery for UHF-RFID systems," in *Proc. IEEE Int. Conf. RFID (RFID)*, May 2022, pp. 41–46.

[7] G. Carroccia and G. Maselli, "Inducing collisions for fast RFID tag identification," *IEEE Commun. Lett.*, vol. 19, no. 10, pp. 1838–1841, Oct. 2015.

[8] H. Guo, C. He, L. Han, N. Chen, and Z. J. Wang, "OCSID: Orthogonal accessing control without spectrum spreading for massive RFID network," *IEEE Internet Things J.*, vol. 8, no. 6, pp. 4329–4338, Mar. 2021.

[9] J. Kaitovic, R. Langwieser, and M. Rupp, "A smart collision recovery receiver for RFIDs," *EURASIP J. Embedded Syst.*, vol. 2013, no. 1, pp. 1–19, Dec. 2013.

[10] J. Kaitovic and M. Rupp, "RFID physical layer collision recovery receivers with spatial filtering," in *Proc. IEEE Int. Conf. RFID Technol. Appl. (RFID-TA)*, Tokyo, Japan, Sep. 2015, pp. 39–44.

[11] H. Salah, H. A. Ahmed, J. Robert, and A. Heuberger, "Multi-antenna UHF RFID reader utilizing stimulated rate tolerance," *IEEE J. Radio Freq. Identificat.*, vol. 1, no. 2, pp. 124–134, Jun. 2017.

[12] X. Tan, H. Wang, L. Fu, J. Wang, H. Min, and D. W. Engels, "Collision detection and signal recovery for UHF RFID systems," *IEEE Trans. Autom. Sci. Eng.*, vol. 15, no. 1, pp. 239–250, Jan. 2018.

[13] H. Salah, H. A. Ahmed, J. Robert, and A. Heuberger, "Maximum likelihood decoding for non-synchronized UHF RFID tags," in *Proc. IEEE Top. Conf. Wireless Sensors Sensor Netw. (WiSNet)*, pp. 89–92, Jan. 2016.

[14] J. Li, H. Wu, and Y. Zeng, "Recovery of collided RFID tags with frequency drift on physical layer," *IEEE/CAA J. Automatica Sinica*, vol. 7, no. 6, pp. 1593–1603, Nov. 2020.

[15] M. Alotaibi, M. Murad, I. A. Tasadduq, S. A. H. Alhuthali, F. R. Al-Osaimi, F. Aldosari, and A. M. Rushdi, "Anti-collision algorithm for identification in precision agriculture applications," *IEEE Access*, vol. 11, pp. 130197–130205, 2023.

[16] R. Jones, S. Yang, R. Penty, and M. Crisp, "MU-MIMO RFID: Proof of concept," in *Proc. IEEE Int. Conf. RFID (RFID)*, Jun. 2024, pp. 1–6.

[17] Z. Dongbo, "A novel radio frequency identification collision resolution method based on statistical learning," *IEEE Access*, vol. 11, pp. 72485–72497, 2023.

[18] C. He, X. Chen, Z. J. Wang, and W. Su, "On the performance of MIMO RFID backscattering channels," *EURASIP J. Wireless Commun. Netw.*, vol. 2012, no. 1, Dec. 2012, Art. no. 357.

[19] J. G. Proakis and M. Salehi, *Digital Communications*, 5th ed., New York, NY, USA: McGraw-Hill, 2007.

[20] F. Fuschini, C. Piersanti, F. Paolazzi, and G. Falciasecca, "Analytical approach to the backscattering from UHF RFID transponder," *IEEE Antennas Wireless Propag. Lett.*, vol. 7, pp. 33–35, 2008.

[21] I. Mayordomo and J. Bernhard, "Implementation of an adaptive leakage cancellation control for passive UHF RFID readers," in *Proc. IEEE Int. Conf. RFID*, Apr. 2011, pp. 121–127.

[22] A. Lazaro, D. Girbau, and D. Salinas, "Radio link budgets for UHF RFID on multipath environments," *IEEE Trans. Antennas Propag.*, vol. 57, no. 4, pp. 1241–1251, Apr. 2009.

[23] C. Angerer, R. Langwieser, and M. Rupp, "RFID reader receivers for physical layer collision recovery," *IEEE Trans. Commun.*, vol. 58, no. 12, pp. 3526–3537, Dec. 2010.

[24] Y. Hua and T. K. Sarkar, "Matrix pencil method for estimating parameters of exponentially damped/undamped sinusoids in noise," *IEEE Trans. Acoust., Speech, Signal Process.*, vol. 38, no. 5, pp. 814–824, May 1990.

[25] H. A. Ahmed, H. Salah, J. Robert, and A. Heuberger, "A closed-form solution for ALOHA frame length optimizing multiple collision recovery Coefficients' reading efficiency," *IEEE Syst. J.*, vol. 12, no. 1, pp. 1047–1050, Mar. 2018.

[26] H. Salah and G. Gaydadjiev, "Alleviating slot collisions in UHF RFID systems," in *Proc. IEEE Sensors*, Oct. 2023, pp. 1–4.

[27] M. F. Khan and M. Tufail, "Comparative analysis of various matrix pencil methods for direction of arrival estimation," in *Proc. Int. Conf. Image Anal. Signal Process.*, Apr. 2010, pp. 496–501.

[28] G. H. Golub and C. V. Loan, *Matrix Computations*. Baltimore, MD, USA: The Johns Hopkins Univ. Press, 2013.

[29] T. Rappaport, *Wireless Communications: Principles and Practice*, 2nd ed., Upper Saddle River, NJ, USA: Prentice-Hall.

[30] H. Salah, J. Robert, H. A. Ahmed, K. Mahmoud, and A. Heuberger, "Theoretical performance evaluation of UHF-RFID systems with multi-antenna maximum-likelihood decoding," *IEEE J. Radio Freq. Identificat.*, vol. 3, no. 2, pp. 108–117, Jun. 2019.

[31] M. Rupp, "On the influence of uncertainties in MIMO decoding algorithms," in *Proc. Conf. Rec. 36th Asilomar Conf. Signals, Syst. Comput.*, vol. 1, 2002, pp. 570–574.

HAMED SALAH received the bachelor's and master's degrees in electrical engineering from Cairo University, in 2005 and 2010, respectively. He is currently pursuing the Ph.D. degree with the Bernoulli Institute for Mathematics, Computer Science and Artificial Intelligence, University of Groningen, with a focus on solving the tags collision problem in UHF RFID systems either using the physical layer or the MAC layer. In 2017, he joined the Broadband and Broadcast Department, Fraunhofer IIS, Erlangen, as a Research Engineer. In 2018, he moved to The Netherlands to join Dialog Semiconductor (Renesas Company) as a DSP System Engineer. Since October 2022, he has been a Hardware System Architect with Synopsys, The Netherlands. He holds six patents and 19 conference and journal papers. His research interests include modem design, UHF RFID systems, hardware implementation of communication systems, and error control codes.

REZA HASSANPOUR received the B.S. degree in computer engineering from Shiraz University, in 1995, the M.S. degree in computer engineering from Tehran Polytechnic University, in 1998, and the Ph.D. degree in computer engineering from Middle East Technical University, in 2003. He is currently an Assistant Professor affiliated with the Computer Science Department, University of Groningen, Groningen, The Netherlands. He has conducted and supervised research works in computer networks, image processing, and machine learning in collaboration with Çankaya University, TU Delft, and Erasmus University Rotterdam.

GEORGI GAYDADJIEV (Senior Member, IEEE) received the M.Sc. degree in electrical engineering and the Ph.D. degree in computer engineering from Delft University of Technology, in 1996 and 2007, respectively. He is currently a Chair Professor of computer architecture with Delft University of Technology and an Honorary Visiting Professor with Imperial College London. He holds three patents, co-authored close to 200 refereed scientific conferences and journal papers, and received three best paper awards. His research interests include computer (system) architecture and micro-architecture, reconfigurable and heterogeneous computing, distributed, and advanced memory systems, design tools and methodologies, low-power architectures, architectural support for compilers, and runtime systems.